Eur. Phys. J. B (2017) 90: 153
DOI: 10.1140/epjb/e2017-80118-4

THE EUROPEAN PHYSICAL JOURNAL B

Regular Article

Coherence and stochastic resonance in a birhythmic van der Pol system

René Yamapi[1,2,3,a], André Chéagé Chamgoué[3], Giovanni Filatrella[4], and Paul Woafo[3]

[1] Fundamental Physics Laboratory, Department of Physics, Faculty of Science, University of Douala, Box 24, 157 Douala, Cameroon
[2] Max Planck Institute for Mathematics in the Sciences, Inselstrasse 22, 04103 Leipzig, Germany
[3] Laboratory of Modeling and Simulation in Engineering, Biomimetics and Prototypes, Faculty of Science, University of Yaoundé I, Box 812, Yaoundé, Cameroon
[4] Dept. of Sciences and Technology and Salerno unit of CNSIM, University of Sannio, via Port'Arsa 11, 82100 Benevento, Italy

Received 25 February 2017 / Received in final form 19 May 2017
Published online 9 August 2017

Abstract. We consider the response to uncorrelated noise and harmonic excitation of a birhythmic van der Pol-type oscillator. This system, as opposed to the standard van der Pol oscillator, is characterized by two stable orbits. The noisy oscillator can be analytically mapped, with the technique of stochastic averaging, onto an ordinary bistable system with a bistable (quasi)potential. The birhythmic oscillator can also be numerically characterized through the diagnostics of coherent resonance and the signal-to-noise-ratio. The analysis shows the presence of noise-induced coherent states, influenced by the different time scales of the oscillator.

1 Introduction

Self oscillatory systems exhibit spontaneous periodic oscillations, i.e. a stable orbit in the phase space. More rarely, one encounters birhythmicity, or the contemporary presence of two stable orbits (limit cycles) for the same set of parameters, as in some biochemical systems [1] or circadian oscillations [2], cell populations [3,4], neuronal dynamics [5], protein dynamics [6]. To model the oscillations, one of the first, and still nowadays prototypal system, is the van der Pol oscillator [7], that has been employed for biological modelling [8] and other oscillations [9–11]. Quite naturally, van der Pol oscillators have been generalized with a higher order polynomial dissipation (that entails multiple stable attractors with different natural frequencies) to be employed as a paradigm for birhythmicity, for example in some enzymatic reactions [10,12–18], or energy harvesting [19]. Noise, that of course is present in real processes, perturbs the periodicity of van der Pol oscillators. In the case of birhythmic systems, noise also induces an hysteretic behavior: the displayed limit cycle depends upon the initial conditions. The transition from an attractor to another is essentially governed by an Arrhenius-type law [20–22] and the effective energy barrier that regulates the escapes depends upon the fluctuation spectrum and the signal (or perturbation) shape. Thus, a van der Pol-type birhythmic system shares the main features of bistable systems [10,23,24]: the presence of two metastable states, an exponential dependence of the lifetime upon the inverse noise intensity, and a mean first passage time across an unstable separatrix. The similarity can be ascribed to the possibility to reduce the averaged system (averaged over the period of the self oscillations) to a standard bistable system governed by a double well quasi-potential (or pseudopotential) [25,26]. This analysis could also take advantage of the nonequilibrium potential constructed on the basis of an extremum principle [27–29]. In fact, it can be postulated that the behavior of the escape times, or more accurately of the mean first passage time through the separatrix between the two attractors, exponentially depends upon a quantity (the quasi-potential, or the effective energy barrier) and it is inversely proportional to the noise intensity [12,18,30]. The quasi-potential approach has also been extended to correlated noise case both driven [31] and undriven [32], that also exhibits stochastic bifurcations [33]. We have made theoretical estimations of the noise thresholds for escape times in van der Pol-type birhythmic system.

We propose to add a sinusoidal drive to such effective bistable potential, i.e. we consider a forced van der Pol type birhythmic system [34] as in some biological systems that are characterized also by a forcing term [35]. When a periodic drive is added to a static, ordinary bistable system characterized by a double well, it is known that the random oscillations between the two (meta)stable solutions induced by noise and the period of the external

[a] e-mail: ryamapi@yahoo.fr

drive can co-operate, producing states that are, in some statistical sense, coherent with the external drive. This is the property exploited in Stochastic Resonance (SR) [36], stochastic signal detection [37,38], and dynamical phase transitions [39]. The interesting phenomenon of SR may appear in a system subject to both random and periodic force [40]. In particular, stochastic resonance is the term used to describe systems in which the presence of input or internal noise provides the optimal output of that system [41,42]. In a nonlinear system, SR ordinarily occurs under three conditions: the presence of a bistable nonlinear system, an applied periodic signal, and the presence of noise. Under these conditions, the response of the system can be similar to the resonance behavior, which is why it is called stochastic resonance. In the van der Pol birhythmic case, the potential is not an actual potential, but a quasi-potential that governs the rare escapes. Moreover, the system has several time scales: the periods of the orbits, the period of the external drive, and the average escape time from the attractors, while in the ordinary analysis of SR the first time scale (the period of the orbits) is absent. It is therefore not obvious that SR can occur, and this is the objective of our research: to investigate if a birhythmic system, where the two states are periodic orbit with an intrinsic time scale, can exhibit a (stochastic) resonance in the presence of noise, as the analogous ordinary bistable systems. Also, we wish to verify if the reduction of the model equation by means of the quasi-potential to a bistable system can also describe the co-operation between the external deterministic drive and the noise effects.

The paper is organized as follows. We first summarize some known properties of van der Pol birhythmic oscillators: in Section 2 we briefly describe the physical model of the periodically driven multi limit-cycle van der Pol oscillator. Section 3 deals with the diagnostic of the coherence between noise and deterministic oscillations in the stochastic birhythmic van der Pol system, to formalize the main tools employed in this work. The original results begin in Section 4, that deals with stochastic resonance-like phenomenon on the birhythmic van der Pol system. In this Section we numerically evaluate the tools employed to quantify the degree of coherence (or anti-coherence). In Section 5, we show that a quasi-potential can be approximately derived, also including the sinusoidal drive. Moreover, we numerically show that the system actually displays SR in the coherent detection mode, at least for some set of parameters. The last section leads to the conclusions.

2 Model of a noisy driven birhythmic system

In this section we set the stage for the studies of the van der Pol like birhythmic system that will be analyzed through the paper. After the model equations have been presented in Section 2.1, it will be shown that the system can be approximately mapped onto a bistable potential for the radius A of the orbits in Section 2.2.

2.1 The model of noisy driven birhythmic system

A stochastic version of a modified van der Pol system that exhibits birhythmicity, is described by the following Langevin equation [12,18,43]:

$$\ddot{x} - \mu(1 - x^2 + \alpha x^4 - \beta x^6)\dot{x} + x = \Gamma(t). \tag{1}$$

Here overdots denote time derivative. The term $\Gamma(t)$ represents an additive Gaussian white noise with amplitude D [40,44]:

$$\langle \Gamma(t) \rangle = 0, \quad \langle \Gamma(t), \Gamma(t') \rangle = 2D\delta(t - t'). \tag{2}$$

The quantities α, β are positive parameters, μ is the parameter of nonlinearity which is restricted to small values, $\mu \ll 1$. Adding an external deterministic drive, equation (1) becomes:

$$\ddot{x} - \mu(1 - x^2 + \alpha x^4 - \beta x^6)\dot{x} + x = E_0 \sin \omega t + \Gamma(t), \tag{3}$$

where E_0 and ω are the amplitude and the frequency of the periodic force, respectively, while the properties of the stochastic term are governed by equation (2).

Equation (3) can be reduced to a nonlinear bistable oscillator in a potential for $E_0 = 0$ [12,14,15,17,18,43]. However, here we assume that the signal $E_0 \sin \omega t$ is small enough ($E_0 \ll 1$), that, in the absence of noise, it cannot force the particle to move from one well to the other. Moreover, we also assume that the periodic signal is slow enough to be considered adiabatic, respect to the time scale of the self excited oscillations (i.e. $\omega \ll 1$).

The system is a nonlinear self-sustained oscillator which possesses more than one stable limit-cycle solution when $\Gamma(t) = 0$ [2,12,18], essential to describe some biological processes. The system exhibits super-harmonic resonance structure, and symmetry-breaking crisis and intermittency. When employed to model biochemical systems like enzymatic-substrate reactions, x in equation (1) is the population of enzyme molecules in the excited polar state [13,15]. The parameters α and β measure the degree of tendency of the system to a ferroelectric instability, and μ is a parameter that effectively refers to strength of nonlinear damping (we refer to [12,18] for more details).

2.2 Analytic considerations

The standard approach to a van der Pol type equations is to approximate the periodic solutions of the free-noise equation (1) with

$$x = A \cos \Omega t. \tag{4}$$

The amplitude A has been found to be independent of the coefficient μ and implicitly given by the relation [18]

$$\frac{5\beta}{64}A^6 - \frac{\alpha}{8}A^4 + \frac{1}{4}A^2 - 1 = 0. \tag{5}$$

The coefficient μ enters in the expression for the frequency Ω, which is implicitly given by the relation

$$\Omega = 1 + \mu^2 \omega_2 + o(\mu^2), \tag{6}$$

where ω_2 is a function of the amplitude A and of the parameters α and β [12,18]. Equation (5), depending on the value of the parameters α and β, gives rise to one or three positive real roots. Thus, for some parameters value, the system exhibits three limit cycle solutions (two stable and one unstable) [12,18,45,46], with different associated frequencies, that is the essence of birhythmicity. The unstable limit cycle represents the separatrix between the basins of attractions of the two stable limit cycles. The shaded area in Figure 1 denotes the region of the parameters α and β where birhythmicity occurs [45,46]. Assuming that the noise intensity is small [18], in the quasiharmonic regime the modified van der Pol equation (1) reduces to the following effective equation that depends on a (quasi)-potential U [25,26]:

$$\frac{dA}{dt} = -\frac{dU(A)}{dA} + \sqrt{\tilde{D}}\zeta_1(t), \tag{7}$$

where $\tilde{D} = D/\omega^2$ and the effective potential $U(A)$ is given by [31]

$$U(A) = \frac{\mu}{128}\left(\frac{5\beta}{8}A^8 - \frac{4\alpha}{3}A^6 + 4A^4 - 32A^2\right) - \frac{\tilde{D}}{2}\ln(A). \tag{8}$$

The barrier of the effective potential ΔU characterizes the escapes from the attractors with limit-cycles A_1 and A_3. In fact, a quasipotential is a Lyapunov function that summarizes the low noise properties of the system with an Arrhenius-like behavior, $\langle T\rangle \propto \exp(\Delta U/D)$ [12,18]. In a bistable system, two barriers characterize the exit times from the two stable states: ΔU_1 and ΔU_3 for the escape from the orbit of radius A_1 and A_3, respectively. As an example, in Tables 1 and 2 we report the energy barriers [12,30] of the multi-limit-cycle associated to the frequencies and amplitudes of the model for some values of the physical parameters α and β. In the shaded region of the parameters plane (α, β) of Figure 1, where two global minima appear, the potential U is symmetric (Tab. 1, $\Delta U_1 \simeq \Delta U_3$, the black line of Fig. 1) or asymmetric (Tab. 2, $\Delta U_1 \gg \Delta U_3$ or $\Delta U_1 \ll \Delta U_3$, the light gray region of Fig. 1) with respect the unstable amplitude A_2 [12,18].

To calculate the statistics of the exit time, i.e. the escape time of the particle from a minimum of the potential, we derive an evolution equation for the Probability Density Function (PDF) of the variable amplitude $A(t)$. The Fokker-Planck equation corresponding to the Langevin equation (7) with δ correlated Gaussian noise sources $\zeta_1(t)$ reads [31,47]

$$\frac{\partial P(A,t)}{\partial t} = \frac{\partial}{\partial A}\left[U' P(A,t)\right] + \frac{\tilde{D}}{2}\frac{\partial^2 P(A,t)}{\partial A^2}. \tag{9}$$

In equation (9), $P(A,t)$ is the PDF of the stochastic process of the limit cycle amplitude $A(t)$. The stationary solution $P(A) = P(A, t \to \infty)$ undergoes a transition from a bimodal to a unimodal (or the opposite, from unimodal to bimodal) distribution by increasing the noise intensity D (see Figs. 5–7 in Ref. [43]). In the absence of additive noise, $D = 0$, the system is conned in one semi-axis ($0 < A < A_2$ or $A_2 < A$, according to the initial condition). Equation (7) gives an estimate for the change in the energy $U(A)$ over the period $2\pi/\omega$ in the quasiharmonic regime. The escape process is depicted in Figure 2 as a jump over an activation barrier $\Delta U_{1\to3}$ (from the leftmost minimum A_1) and $\Delta U_{3\to1}$ (from the rightmost minimum A_3) [12,18]. The characteristics height can be controlled by the variation of the parameters α and β [30]. The noisy birhythmic van der Pol equation (1) can be characterized through the distribution $P(T)$ of the escape times (denoted by T_i) from the two wells of potential U. The probability for the system to *hop* between the potential wells is defined through noise dependent Kramers rate [47,48], which is the inverse of the average escape time $\langle T\rangle$. The quantities $\langle T_{1,3}\rangle$ [18,30] for small noise intensity $D < \Delta U_{\rm i}$ are given by (here the primes refer to differentiation respect to the radius A):

$$\langle T_1(1\to3)\rangle = \sqrt{\frac{2\pi}{U''(A_1)|U''(A_2)|}}\exp\left(\frac{\Delta U_{1\to3}}{\tilde{D}}\right), \tag{10}$$

that describes the transition of the system from attractor with limit-cycle amplitude A_1 (left side potential well) to attractor with limit-cycle amplitude A_3 (right side potential well). A similar equation holds for the reverse passage, i.e.

$$\langle T_3(3\to1)\rangle = \sqrt{\frac{2\pi}{U''(A_3)|U''(A_2)|}}\exp\left(\frac{\Delta U_{3\to1}}{\tilde{D}}\right). \tag{11}$$

The quantities (10) and (11) measure the relative stabilities pertaining to the attractors with limit cycle amplitude A_1 and A_3 through the resident time given by the relation [18,30]:

$$R_{1,3} = \frac{T_{1,3}}{T_1 + T_3}. \tag{12}$$

The characteristics of the stability properties through equation (12) in a modified van der Pol oscillator (1) are strongly influenced by both the nonlinear coefficients α, β and the noise intensity D [30]. An escape is counted if the amplitude of the system A is greater than the separatrix amplitude A_2 for left to right escape. Analogously, if the amplitude is less than the separatrix one counts the reversal passage from right to left. In the absence of noise, the system would remain confined to its initial state. In the presence of noise, transitions eventually occur, and the two-state output evasion is a random distributed sequence. However, a birhythmic system with an intrinsic time scale there is the possibility that the noise cooperates with the internal time scales. The measure of the degree of cooperation is the subject of the next section.

3 Diagnostics of coherent resonance and stochastic resonance

To characterize the birhythmic system one can analyze the dynamics of the radius A of the oscillations, as per equation (4). A principal question is: does the quasi-potential

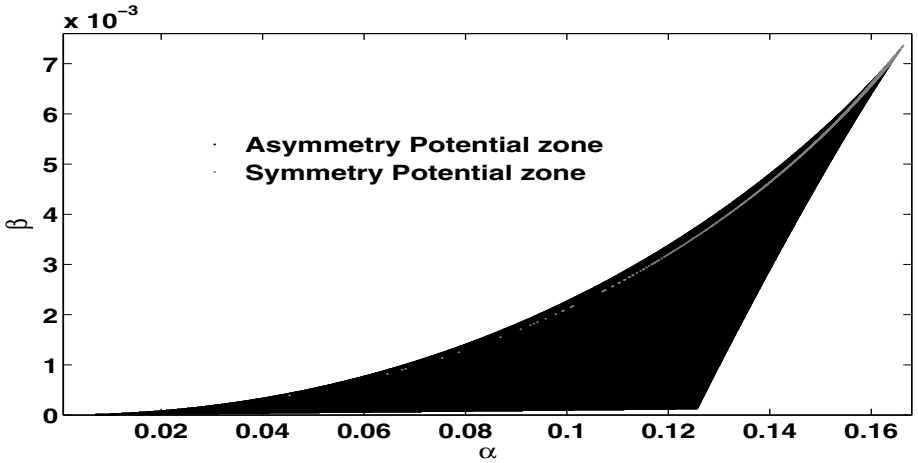

Fig. 1. Parameters domain for the existence of a single limit cycle (white area) and three limit cycles (shadowed area). The black zone is the domain of asymmetric potential, whereas the grey area is the region of symmetric potential. The nonlinear parameter reads $\mu = 0.001$.

Table 1. Amplitudes, frequencies and energy barriers of the limit cycles for the symmetric potential. All data refer to the case $\mu = 0.001$.

$S_i = (\alpha, \beta)$	Analytical amplitudes	Numerical frequencies	Energy barriers $\Delta U_{1,3}$
$S_1 = (0.0675, 0.0009)$	$A_1 = 2.1730001$	$\Omega_1 = 1.0000003$	$\Delta U_1 = 6.8055 \times 10^{-3}$
	$A_2 = 6.3245003$	$\Omega_2 = unstable$	
	$A_3 = 8.6760004$	$\Omega_3 = 0.9999923$	$\Delta U_3 = 6.8055 \times 10^{-3}$
$S_2 = (0.12, 0.0032)$	$A_1 = 2.4200001$	$\Omega_1 = 0.9999999$	$\Delta U_1 = 6.25 \times 10^{-4}$
	$A_2 = 4.4720002$	$\Omega_2 = unstable$	
	$A_3 = 5.8430003$	$\Omega_3 = 0.9999923$	$\Delta U_3 = 6.25 \times 10^{-4}$
$S_3 = (0.1476, 0.0053)$	$A_1 = 2.6905001$	$\Omega_1 = 0.9999999$	$\Delta U_1 = 8.671 \times 10^{-5}$
	$A_2 = 3.8525002$	$\Omega_2 = unstable$	
	$A_3 = 4.7405002$	$\Omega_3 = 0.9999986$	$\Delta U_3 = 8.767 \times 10^{-5}$
$S_4 = (0.16, 0.00658)$	$A_1 = 2.9520001$	$\Omega_1 = 0.9999998$	$\Delta U_1 = 1.035 \times 10^{-5}$
	$A_2 = 3.5965002$	$\Omega_2 = unstable$	
	$A_3 = 4.1535002$	$\Omega_3 = 0.9999990$	$\Delta U_3 = 1.101 \times 10^{-5}$
$S_5 = (0.1547, 0.006)$	$A_1 = 2.8145001$	$\Omega_1 = 1.000$	$\Delta U_1 = 3.384 \times 10^{-5}$
	$A_2 = 3.7085002$	$\Omega_2 = unstable$	
	$A_3 = 4.4240002$	$\Omega_3 = 0.9999990$	$\Delta U_3 = 3.368 \times 10^{-5}$
$S_6 = (0.1635, 0.007)$	$A_1 = 3.0925001$	$\Omega_1 = 1.000$	$\Delta U_1 = 2.377 \times 10^{-6}$
	$A_2 = 3.5280002$	$\Omega_2 = unstable$	
	$A_3 = 3.9190002$	$\Omega_3 = 0.9999992$	$\Delta U_3 = 2.445 \times 10^{-6}$

Table 2. Amplitudes, frequencies and energy barriers of the limit cycles for the asymmetric potential. All data refer to the case $\mu = 0.001$.

$AS_i = (\alpha, \beta)$	Analytical amplitudes	Numerical frequencies	Energy barriers $\Delta U_{1,3}$
$AS_1 = (0.065, 0.0009)$	$A_1 = 2.1640001$	$\Omega_1 = 1.000$	$\Delta U_1 = 9.0101 \times 10^{-3}$
	$A_2 = 7.0255003$	$\Omega_2 = unstable$	
	$A_3 = 7.8425004$	$\Omega_3 = 0.9999992$	$\Delta U_3 = 0.2667 \times 10^{-3}$
$AS_2 = (0.145, 0.005)$	$A_1 = 2.6605001$	$\Omega_1 = 1.000$	$\Delta U_1 = 0.982 \times 10^{-4}$
	$A_2 = 3.8305002$	$\Omega_2 = unstable$	
	$A_3 = 4.9645002$	$\Omega_3 = 0.9998368$	$\Delta U_3 = 2.0332 \times 10^{-4}$
$AS_3 = (0.154, 0.006)$	$A_1 = 2.7860001$	$\Omega_1 = 1.000$	$\Delta U_1 = 5.192 \times 10^{-5}$
	$A_2 = 3.8820002$	$\Omega_2 = unstable$	
	$A_3 = 4.2695002$	$\Omega_3 = 0.9999990$	$\Delta U_3 = 0.5477 \times 10^{-5}$
$AS_4 = (0.1638, 0.007)$	$A_1 = 3.1870002$	$\Omega_1 = 1.000$	$\Delta U_1 = 0.131 \times 10^{-6}$
	$A_2 = 3.3430002$	$\Omega_2 = unstable$	
	$A_3 = 4.0125002$	$\Omega_3 = 0.9999992$	$\Delta U_3 = 9.487 \times 10^{-6}$

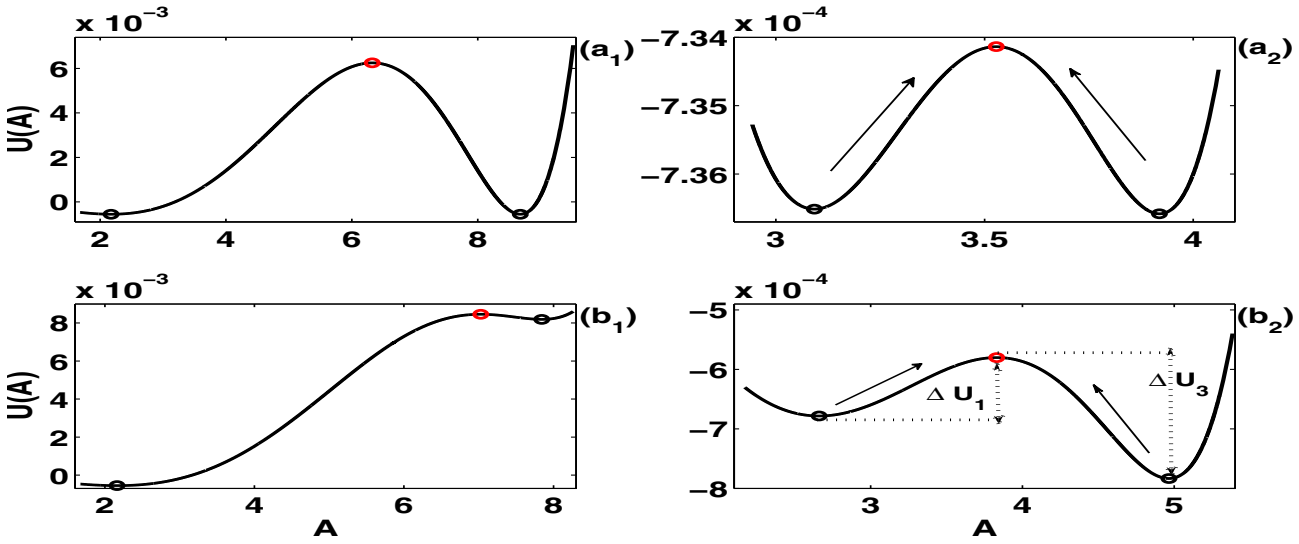

Fig. 2. The quasi-potential energy of a bistable system and an illustration of the escape process. The minima are at A_1 and A_3 (black circle), the maximum at A_2 (red circle); in the stochastic averaging reduction each point represents an orbit amplitude, see equation (1), of frequency given by equations (5) and (6). A switching from A_1 to A_3 and vice versa over the energy barrier ΔU_1 ($A_1 \to A_3$) and ΔU_3 ($A_3 \to A_1$) can occur under the influence of noise. In all panels $\mu = 0.001$, the other parameters are: ($a_{1,2}$): $\alpha = 0.0675$, $\beta = 0.0009$ and $\alpha = 0.1635$, $\beta = 0.007$, corresponding to the symmetric case, Table 1, cases S_1 and S_6; ($b_{1,2}$): $\alpha = 0.0650$, $\beta = 0.0009$ and $\alpha = 0.145$, $\beta = 0.005$, corresponding to the asymmetric case, Table 2, cases AS_1 and AS_2.

approximation give a bona fide bistable potential? Put it in other words, we ask if the system evolution has the same features of the dynamics of a particle subject to an ordinary bistable potential, and if the entrained oscillations give rise to the same type of resonances expected in ordinary potentials. We thus summarize the most common diagnostics of stochastic coherence and resonance. Coherence Resonance (CR) refers to the appearance of coherent oscillations in a dynamical system in the presence of noise. In particular it can refer to the appearance of coherent behaviour at an optimal noise strength, i.e. to the emergence of orderly behaviour in the system due to the noise presence (the FitzHugh – Nagumo model [49] probably being the first prototype model for CR). We propose to extend the same diagnostic used by Pikovski and Kurths [49] to the stochastic birhythmic van der Pol model to detect the occurrence of CR. Also SR is assessed in the literature with several quantities, such as the residence-time distribution density of a particle in one of the potential wells [37], the spectral power amplitude [38,50], the hysteresis loop area (HLA) [51] and the Signal-to-Noise Ratio (SNR) [16], to name few. When adding noise any of the above tools measures an improvement of the signal quality, one speculates that the noise has induced stochastic resonance, as we shall discuss in the following.

3.1 Tools to quantify coherent resonance

To quantitatively characterize the regularity of a system in the presence of noise, let us begin with the normalized Auto-Correlation Function (ACF), namely:

$$C(\tau) = \frac{\langle \widetilde{A}(t)\widetilde{A}(t-\tau)\rangle}{\langle \widetilde{A}^2\rangle}, \quad \widetilde{A} = A - \langle A\rangle. \tag{13}$$

Noise induced coherence can also be characterized by a decay rate of the ACF, i.e. by a Correlation Time (CT) [22,49], defined as

$$\tau_{\rm cor} = \frac{1}{{\rm Var}(A(t))} \int_0^{+\infty} C^2(\tau) d\tau, \tag{14}$$

where ${\rm Var}(A(t))$ is the variance of the amplitude $A(t)$.

Considering $A(t)$ as a transmitted signal, the correlation time is an indicator of the regularity or the coherence of the signal. The highest value gives the best noise intensity necessary for Coherence Resonance (CR) if, as noise is increased, the CT reaches a maximum. The idea is to compute different correlation times for different noise intensities and find the optimal intensity of the noise D_c. Another way to quantify CR is to compute $\tau_{\rm cor}$, to check if there is a noise level above which the random term destroys the coherence. In reference [49] it was also introduced the analysis of the standard deviation of the escape times as a noise-signal ratio, R_{ET}. Coherence resonance is then quantified in terms of the parameter $R_{\rm ET}$, named Coefficient of Variation (CV):

$$R_{ET} = \frac{\sqrt{\langle T^2\rangle - \langle T\rangle^2}}{\langle T\rangle}, \tag{15}$$

here $\langle T\rangle$ is the mean, and $\langle T^2\rangle - \langle T\rangle^2$ is the variance of the ETs from one stable orbit to the other through the unstable orbit of amplitude A_2. A perfectly ordered system, with escapes occurring at a regular pace, entails $R_{ET} = 0$. Thus, a minimum of R_{ET} also signals the presence of CR.

The escape times can also be described by means of an effective noise intensity defined as [52,53]:

$$D_{\text{eff}} = \frac{R_{ET}^2}{2\langle T\rangle} \tag{16}$$

that, at variance with CV, should exhibit a maximum when coherence is enhanced.

3.2 Tools to quantify stochastic resonance

The measures introduced so far characterize the intrinsic order of the escape times. In some circumstances, when the system is investigated as a detector, it is interesting to compare how the response of the system is influenced by a periodic (sinusoidal) drive [37,38]. In these cases, one wants to measure the response of the system in the presence of the input $E_0 \sin \omega t$ compared to the case when the system is solely subject to a random term, that is the Signal to Noise-Ratio (SNR) [54–56]. To characterize SR one can numerically calculate SNR using the mean square displacement in the presence of a weak signal and the mean square displacement induced by noise. To do so, one defines the Root Mean Square (RMS) displacement:

$$\text{RMS} = \int A(t)A(t-t')dt' \tag{17}$$

and then SNR can then be defined as the ratio of the RMS in the presence of a mixture of noise and a signal with the case of pure noise:

$$\text{SNR} = \frac{RMS(E \neq 0, D \neq 0)}{RMS(D \neq 0)}. \tag{18}$$

SR appears to be counterintuitive, inasmuch it seems to imply that the signal quality does not deteriorate as the random noise is increased. In fact, for nonlinear systems with an input signal, only in special circumstances increasing the random noise can actually improve the detection of the corrupted signal [42].

4 Stochastic like-resonance of birhythmic van der Pol systems

In this section, we discuss the application of the concepts illustrated in Section 3 to the birhythmic van der Pol model discussed in Section 2.1. The purpose is to investigate the effect of noise on the driven birhythmic system governed by equation (1). The two-dimensional system is reduced to a one-dimensional system through the instantaneous amplitude

$$A \equiv \sqrt{x^2(t) + \dot{x}^2(t)}, \tag{19}$$

that is the counterpart of the approximation (4).

Figures 3a and 3b display the ACF, $C(\tau)$ as per equation (13), for six different values of noise amplitude and for two different sets of parameters α and β, when the quasi-potential is symmetric or asymmetric, respectively (see Tabs. 1 and 2). In these figures the drive term is absent, $E_0 = 0$, equation (1).

For the set (a) the autocorrelation increases at intermediate values of noise, namely $D \simeq 10^{-4}$, see Figure 3a$_3$. Similarly, for the set (b), in Figure 3b$_2$ on observes an increase at $D \simeq 5 \times 10^{-5}$. It is thus noticeable that a resonance occurs also when $E_0 = 0$ in equation (1), for the absence of an obvious periodic drive. However, the presence of two periodic attractors clearly gives the possibility of the noise induced escapes and synchronization with the deterministic period proper of the attractors. It is therefore decisive to compare the noise intensity at which a resonance occurs with the time-scale given by the quasi-potential, as in equation (10). For the noise intensity of Figure 3a$_2$, $D = 10^{-4}$, equation (10) with the parameter values of Table 1 gives an escape time of about $\langle T(1 \to 3)\rangle \approx 10^4$. One can conclude that the dominating time scale is given by the activation energy, as derived from the quasipotential (8), and not by the period of the van der Pol oscillations (that is $\approx 2\pi$, see Tabs. 1 and 2).

Also the CT, given by equation (14), can be used as a measure of the coherence [49]. If noise can cooperate with the deterministic oscillations, we expect that τ_{cor} is maximized at non-zero noise intensity. The dependence of this quantity on the noise amplitude is presented in Figure 4. At variance with reference [49], the CT has a clear minimum at the critical noise amplitude. Panel (a) refers to the symmetrical potential, while panel (b) refers to the asymmetric case. The presence of a minimum is a clear signature of anti-coherence resonance [57]. The minimum value $\tau_{\text{cor,min}}$ measures the strength of the anti-correlation between the residence time in the two stable states. At the minimum the critical noise amplitude D_c reads, for the panel (a) $D_c = 1.77$, while in panel (b) it reads $D_c = 2.07$. An estimate of the escape time through equation (10) is only valid for vanishing noise [25,26], so it cannot be used for $D \approx 1$. However, numerical simulations of the full equation (1) give an escape time of about $T \approx 10$, i.e. it matches the oscillation period of the attractors. We conclude that CT (measured through τ_{cor}), is most sensitive to periodic oscillations underlying the van der Pol birhythmic system, oscillations that are neglected by the stochastic averaging. We also conclude that the ACF ($C(\tau)$ in Fig. 3) and the CT (τ_{cor} in Fig. 4) are sensitive to different time scales contained in the system.

In the analysis of the ET it is tempting to employ the oscillation frequencies to have an estimate of the deterministic oscillation periods (the ratio is that in the actual system, at variance with the reduced quasi-potential, *something* oscillates at the frequency Ω). Using the approximated relationship between the external drive frequency and the escape time for time scale matching SR [37]

$$\langle T\rangle = \frac{\pi}{\Omega}. \tag{20}$$

We therefore seek for SR at noise levels where the average escape is the inverse of the van der Pol oscillation period.

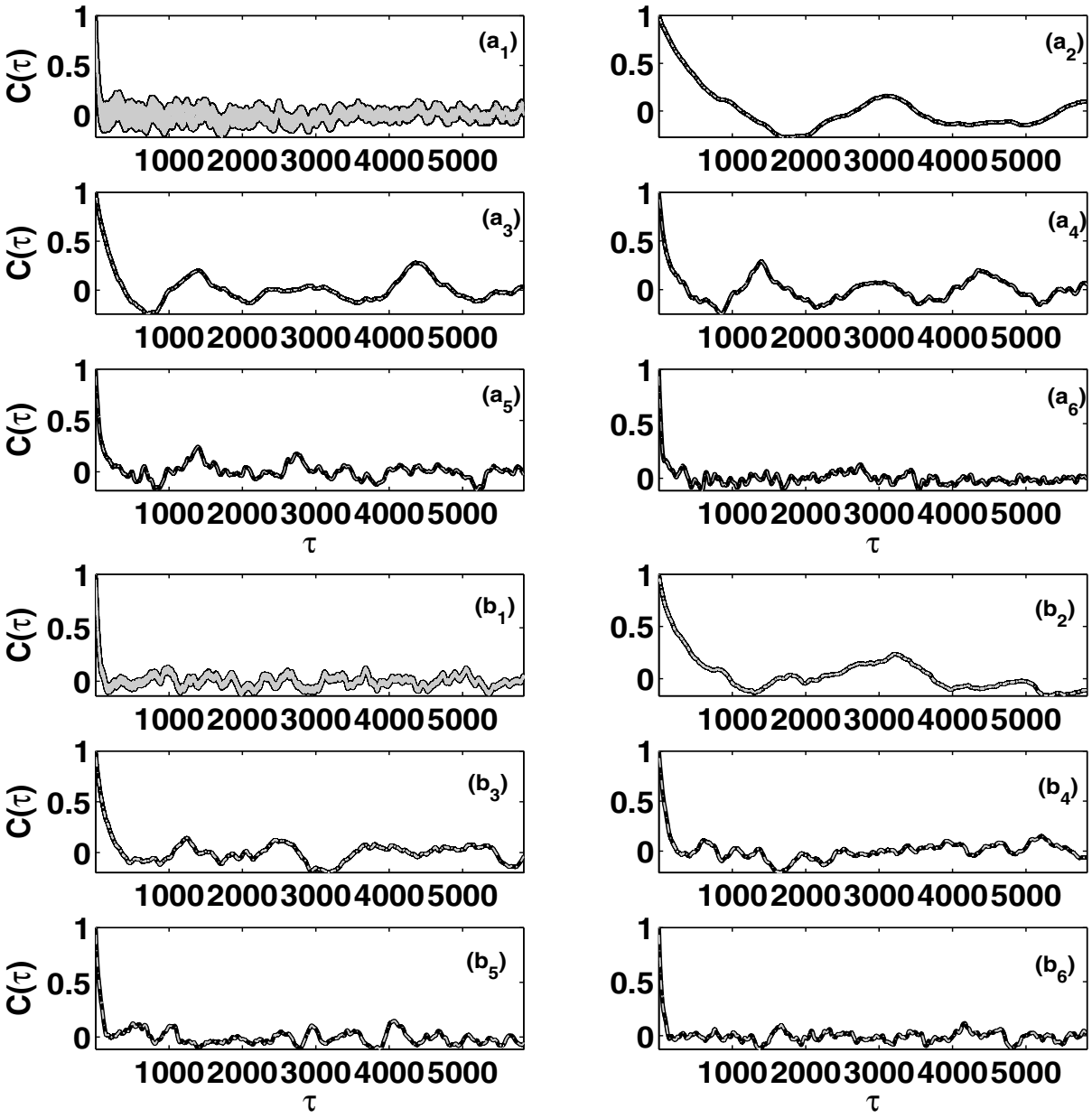

Fig. 3. The autocorrelation function $C(\tau)$ for different noise amplitudes, see equation (13). The set (a_i) (top panels) corresponds to the symmetric case, S_5, see Table 1, with $\alpha = 0.1547$, $\beta = 0.006$, while the set (b_i) (bottom panels) corresponds to the asymmetric case, AS_3, see Table 2, with $\alpha = 0.154$, $\beta = 0.006$. The subscripts refer to the noise intensity: $(a,b)_1$: $D = 1 \times 10^{-5}$, $(a,b)_2$: $D = 5 \times 10^{-5}$, $(a,b)_3$: $D = 1 \times 10^{-4}$, $(a,b)_4$: $D = 2.5 \times 10^{-4}$, $(a,b)_5$: $D = 5 \times 10^{-4}$, and $(a,b)_6$: $D = 1 \times 10^{-3}$. In all panels we have set the parameter $\mu = 0.001$, $E_0 = 0$.

The normalized fluctuations of the ETs distribution, equation (15), has been employed to quantity the effect of noise on the system (3) in Figures 5a_{1-4}. The CV changes of several orders of magnitude, thus indicating sharp variations of the degree of coherence in response to noise changes. The strongly nonlinear behaviour with evident peaks (or dips) at special values of the noise intensity D (see Tabs. 3 and 4) for both the passages from the inner orbit to the outer (R_{ET_1}) and from the outer to the inner orbit (R_{ET_1}). For both the symmetric quasi-potential, Figures 5a_{1-2} and the asymmetric quasi-potential, Figures 5a_{3-4}, it appears that the escapes become suddenly very disordered at $D \simeq 2.971, 5.942, 16.83$, and 21.79. It is evident that at these noise values the noise can cooperate with the intrinsic oscillations of the van der Pol system, giving rise to a significant reduction of the variance of the ET from the inner orbit, and conversely to greatly increase the disorder in the escapes from the other well.

Tables 3 and 4 provide the values D at the peaks (dips), and the corresponding escape time $\langle T \rangle$, this shows the decreasing of $\langle T_1 \rangle$ and the increasing of $\langle T_3 \rangle$.

The phenomenon is confirmed by the behavior of the effective diffusion D_{eff}, given by equation (16), that can be considered as an alternative measure of SR. As cit

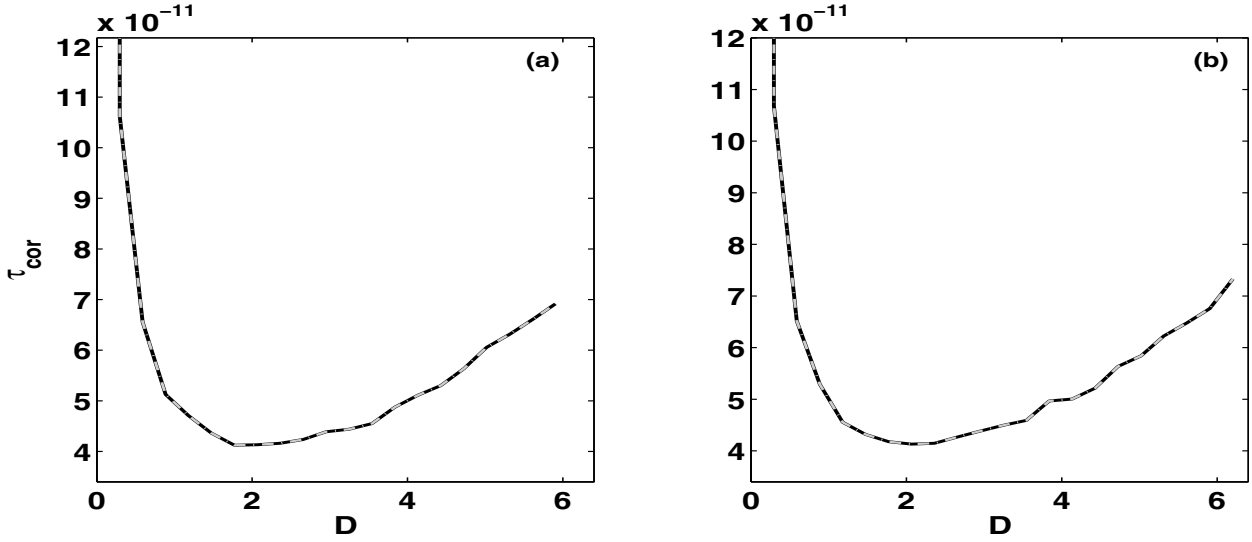

Fig. 4. Correlation times τ_{corr} as a function of the noise intensity D. The grey line dot curve is the correlation times from right to left, whereas the black curve is for left to right. The parameter are $\mu = 0.001$, (a): $\alpha = 0.1547$, $\beta = 0.006$ for symmetric case, and (b): $\alpha = 0.154$, $\beta = 0.006$ for asymmetric case. In all panels we have set the parameter $\mu = 0.001$, $E_0 = 0$.

Table 3. Pronounced values of the averaged escape times $\langle T_1(A_1 \to A_3)\rangle$ and $\langle T_3(A_3 \to A_1)\rangle$ for the case of symmetry potential.

D	$\langle T_1(A_1 \longrightarrow A_3)\rangle$	$\langle T_3(A_3 \longrightarrow A_1)\rangle$
2.971	0.311202344163790	1.93331429910557
5.942	$9.442004022060120 \times 10^{-2}$	0.933103116355772
16.83	$6.564115778189560 \times 10^{-2}$	1.81793686513413
21.79	$6.156881219055681 \times 10^{-2}$	2.50400902740351

Table 4. Pronounced values of the averaged escape times $\langle T_1(A_1 \to A_3)\rangle$ and $\langle T_3(A_3 \to A_1)\rangle$ for the case of asymmetry potential.

D	$\langle T_1(A_1 \longrightarrow A_3)\rangle$	$\langle T_3(A_3 \longrightarrow A_1)\rangle$
2.971	0.315577448605940	1.82583134563407
5.942	0.215271280189222	1.60995055543023
16.83	0.127857473503098	1.69808016157355
21.79	0.113841745789081	1.83781953721047

is evident in Figures 5b$_{1-4}$, the effective diffusion closely follows the escape times behavior.

To further investigate the appearance of different timescales in signal enhancement we include the effects of the drive term E_0 at frequency ω in the next section.

5 Effects of a periodic signal on the birhythmic system

In this section we extend the analytic treatment of the noisy system (1) to the case of an applied periodic drive (3). To do so, we restrict the frequency of the drive to be close to the natural frequency of the van der Pol oscillator.

5.1 Analytical treatment of the stochastic driven van der Pol birhythmic system

We consider the driven modified van der Pol system (3), where we assume that the deterministic source can oscillate harmonically close to the natural frequency, i.e. $\omega = \Omega + \nu$, with $\nu \ll 1$. To analyse equation (3), we introduce two variables $y_1(t)$, $y_2(t)$ related to the $(x, \dot{x})$ phase-space, that rotate at the frequency of the drive ω:

$$y_1 = x\cos\omega t - \frac{\dot{x}}{\omega}\sin\omega t, \tag{21a}$$

$$y_2 = x\sin\omega t + \frac{\dot{x}}{\omega}\cos\omega t. \tag{21b}$$

We use the Krylov-Bogoliubov averaging method [58], as in reference [59], with the assumption that friction parameter μ is not too large ($\mu \ll 1$), to obtain the following basic (averaged) equations:

$$\dot{y_1} = P_1(y_1, y_2) - \xi_1(t), \tag{22a}$$

$$\dot{y_2} = P_2(y_1, y_2) + \xi_2(t), \tag{22b}$$

where

$$P_1(y_1, y_2) = \nu y_2 + \frac{\mu y_1}{2} \times \left[1 - \frac{1}{4}(y_1^2 + y_2^2) + \frac{\alpha}{8}(y_1^2 + y_2^2)^2 - \frac{5\beta}{64}(y_1^2 + y_2^2)^3\right] - \frac{\mu E_0}{2\omega},$$

$$P_2(y_1, y_2) = -\nu y_1 + \frac{\mu y_2}{2} \times \left[1 - \frac{1}{4}(y_1^2 + y_2^2) + \frac{\alpha}{8}(y_1^2 + y_2^2)^2 - \frac{5\beta}{64}(y_1^2 + y_2^2)^3\right].$$

Here, $\nu \sim (\Omega^2 - \omega^2)/(2\omega)$ and the excitations $\xi_1(t)$ and $\xi_2(t)$ are two independent normalized Gaussian white

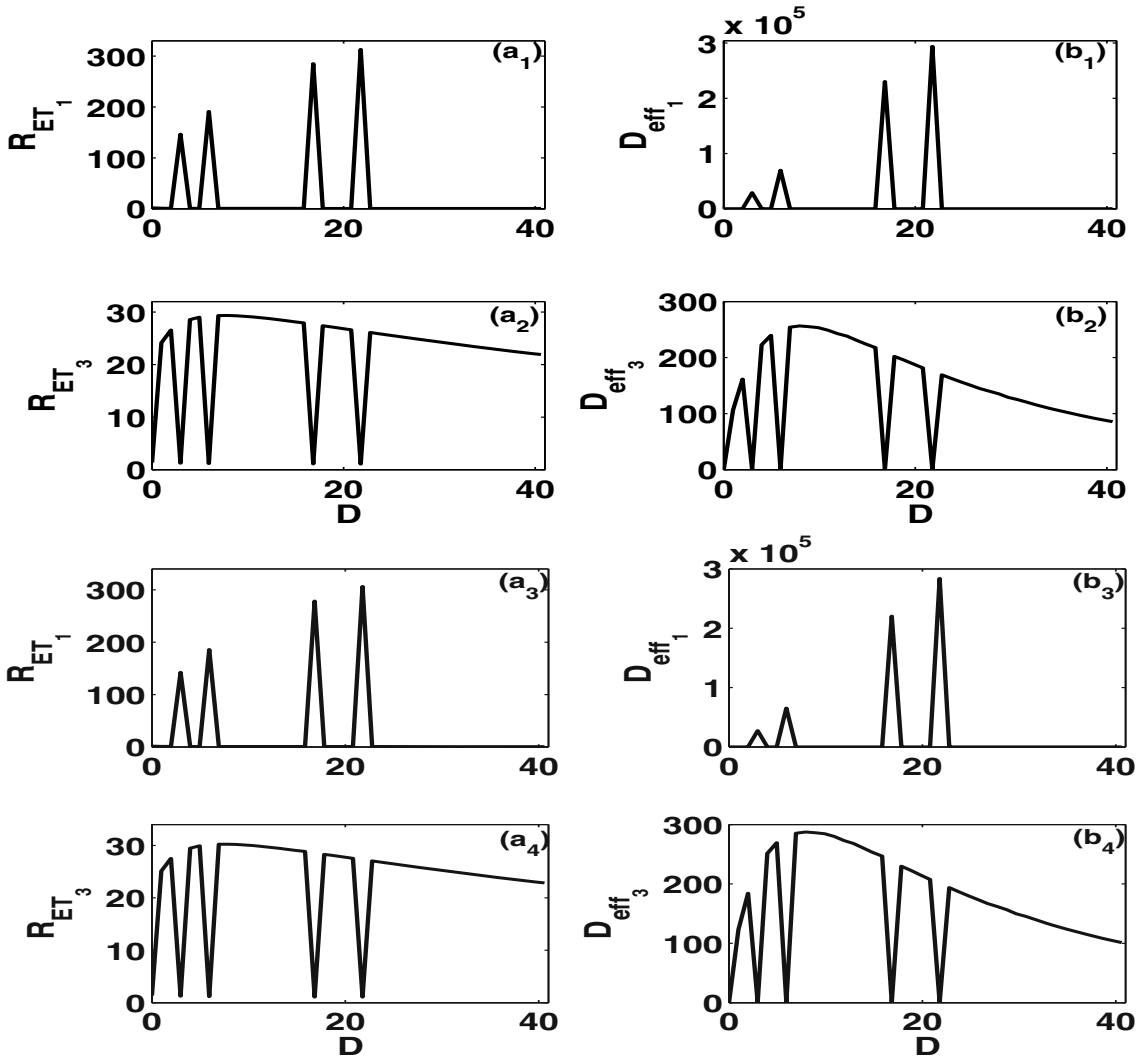

Fig. 5. (a_i) Coefficient of variation R_{ET} and (b_i) effective diffusion constant $D_{\rm eff}$ versus the noise amplitude D for the undriven birhythmic van der Pol system. Both quantities clearly exhibit a strong change for special values of the noise, $D \simeq 2.971, 5.942, 16.83$, and 21.79. The subscripts 1 and 3 refer the escapes from the inner (A_1) or the outer (A_3) orbits, respectively. The top panels, ($a_{1,2}$) and ($b_{1,2}$) correspond to $\alpha = 0.1547$, $\beta = 0.006$, the symmetric quasi-potential case. The lower panels ($a_{3,4}$) and ($b_{3,4}$) correspond to $\alpha = 0.154$, $\beta = 0.006$, the asymmetric potential case. In all panels we have set the parameter $\mu = 0.001$, $E_0 = 0$.

noises with intensity $\widetilde{D} = \frac{D}{\omega^2}$. The associated PDFs of y_1 and y_2 are

$$\frac{\partial p}{\partial t} = -\frac{\partial J_1}{\partial y_1} - \frac{\partial J_2}{\partial y_2}, \tag{23}$$

where

$$J_1 = P_1(y_1, y_2)p + \frac{\widetilde{D}}{2}\frac{\partial p}{\partial y_1}, \text{ and } J_2 = P_2(y_1, y_2)p - \frac{\widetilde{D}}{2}\frac{\partial p}{\partial y_2}.$$

Here, J_1 and J_2 are the probability currents or stationary state probability currents, for the Fokker Planck equation (22), which are not in general constants. However, for certain conditions on P_1 and P_2 [22], in the steady state J_1 and J_2 vanish. Under these conditions, J_1 and J_2 can be derived from a potential V, as

$$P_1 = -\frac{\partial V}{\partial y_1}, \quad P_2 = -\frac{\partial V}{\partial y_2}. \tag{24}$$

The potential V exists if the following potential condition holds [60]:

$$\frac{\partial P_1}{\partial y_2} - \frac{\partial P_2}{\partial y_1} = 0. \tag{25}$$

For our problem one finds

$$\frac{\partial P_1}{\partial y_2} - \frac{\partial P_2}{\partial y_1} = 2\Delta, \tag{26}$$

where $\Delta \sim \nu$. At this stage, two cases can be considered: case $\Delta = 0$ and case $\Delta \neq 0$.

The optimal situation is the case $\Delta = 0$, in which the harmonic forcing frequency is locked to the frequency of the multi-limit cycle oscillation, i.e. $\omega \sim \Omega$. equation (22) represents an overdamped version of two coupled anharmonic oscillator [61,62]. In the absence of detuning

Table 5. Characteristics limit of driving amplitude for bistability.

(α, β)	Phase	Limit of E_0
$\alpha = 0.145, \beta = 0.005$	$\phi = -\frac{\pi}{2}$	$E_0 < 0.2564$
$\alpha = 0.145, \beta = 0.005$	$\phi = \frac{\pi}{2}$	$E_0 < 0.5764$
$\alpha = 0.154, \beta = 0.006$	$\phi = -\frac{\pi}{2}$	$E_0 < 0.1484$
$\alpha = 0.154, \beta = 0.006$	$\phi = \frac{\pi}{2}$	$E_0 < 0.0429$

($\Delta = 0$) and noise terms the potential of the two coupled anharmonic oscillators is

$$V(y_1, y_2) = -\mu \left(\frac{1}{4}(y_1^2 + y_2^2) - \frac{1}{32}(y_1^2 + y_2^2)^2 + \frac{\alpha}{96}(y_1^2 + y_2^2)^3 - \frac{5\beta}{1024}(y_1^2 + y_2^2)^4 - \frac{E_0}{2\omega} y_1 \right). \quad (27)$$

Next we transform the potential (27), into the amplitude and phase variables setting $y_1 = A\sin(\phi)$, $y_2 = A\cos(\phi)$. This leads to:

$$V(A, \phi) = -\mu \left(\frac{1}{4}A^2 - \frac{1}{32}A^4 + \frac{\alpha}{96}A^6 - \frac{5\beta}{1024}A^8 - \frac{E_0}{2\omega} A\sin(\phi) \right). \quad (28)$$

In the new variables (A, ϕ), the parameters μ, α and β are fixed as in Figure 2. For this choice, depending on excitation force amplitude E_0, the potential has two or four minima and is a two or a four well potential. Stationary oscillations under deterministic excitation are obtained setting:

$$\begin{cases} \frac{\partial V}{\partial \phi} = 0 \\ \frac{\partial V}{\partial a} = 0 \end{cases} \Leftrightarrow \begin{cases} \cos(\phi) = 0, \\ 5\beta A^7 - 8\alpha A^5 + 16A^3 - 64A + \frac{64E_0}{\omega}\sin(\phi) = 0, \end{cases} \quad (29)$$

for given values of α and β. The amplitudes are plotted in Figure 6 as a function of the excitation E_0, for ϕ ($\phi = -\frac{\pi}{2}$ and $\phi = \frac{\pi}{2}$), at different frequencies of the external drive. It is observed that the bistabilities zone widens with the increase of E_0. In Figure 6, the black lines are the stable amplitude combined with both phases, for $\phi = -\pi/2$ in Figure 6b$_1$, and $\phi = \pi/2$ (in Fig. 6b$_2$). The gray curves represent the unstable amplitude. The limit of the amplitude excitation to permit bistability are summarized in Table 5 for the frequency of excitation $\omega = 1$.

Below the critical value of E_0 of Table 5 the following equations for A and ϕ characterize the escapes:

$$\dot{A} = -\frac{\mu}{128}(5\beta A^6 - 8\alpha A^4 + 16A^2 - 64)a - \frac{\mu E_0}{2\omega}\sin(\phi) + \frac{\tilde{D}}{2a} - \xi_1(t), \quad (30a)$$

$$\dot{\phi} = \Delta - \frac{\mu E_0}{2A\omega}\cos(\phi) + \xi_2(t). \quad (30b)$$

The stability analysis of equations (30a) and the of the related potential V given by equation (28) show that only the points $(A_i, \phi = -\pi/2)$ are stable. In many noisy systems the method leads to a one-dimensional approximation to the response amplitude that significantly simplifies the solution procedure. However, the simplified equation is coupled with the phase equation and of solution of the PDF of amplitude and phase is not possible in general. Thus, to characterize the escape time, we consider equation (30a) and replace the terms containing ϕ by the corresponding deterministic values. This amounts to set $\phi = -\pi/2$ in equation (30a), that leads to

$$\dot{A} = -\frac{\mu}{128}(5\beta A^6 - 8\alpha A^4 + 16A^2 - 64)A + \frac{\mu E_0}{2\omega} + \frac{\tilde{D}}{2A} - \xi_1(t). \quad (31)$$

Therefore, the equation for the amplitude A is independent of ϕ. The deterministic potential corresponding to equation (31) reads

$$V(A) = -\mu \left(\frac{1}{4}A^2 - \frac{1}{32}A^4 + \frac{\alpha}{96}A^6 - \frac{5\beta}{1024}A^8 + \frac{E_0}{2\omega}A \right). \quad (32)$$

It has two stable states and an unstable state; under the condition resumed in Table 5, namely, it is bistable. The reduced deterministic potential $V(A)$, as a function of amplitude a for different values of the amplitude E_0, is plotted in Figure 7. One can see that for the outer oscillation amplitude the potential well deepens, the inner potential well becomes shallow as E_0 increases. Through equation (32) one can derive the behavior of the potential barriers ΔV_1 and ΔV_3, that are shown in Figure 8 as a function of the periodic signal intensity E_0. It is evident that increasing of E_0 above some limit (reported in Tab. 5), the leftmost potential well, associated to the inner orbit, disappears. Asymmetric forms are still observed according to the value of the control parameters E_0. This gives rise to the possible switching over the potential well in the presence of noisy excitation. To reveal how the periodic drive affect the escape times process and their distribution of the escape times on right potential well and the left potential well of the system equation (31).

The Fokker-Planck equation corresponding to the reduced equation (31) can be written as

$$\frac{\partial p}{\partial t} = \frac{\partial}{\partial A}\left[V'_{\text{eff}} p\right] + \frac{\tilde{D}}{2}\frac{\partial^2 p}{\partial A^2}. \quad (33)$$

Hence, the stationary solution of equation (33) is

$$P_{\text{st}}(a) = N_{\exp}\left(-\frac{V_{\text{eff}}(A)}{2\tilde{D}} \right), \quad (34)$$

with N being a normalization constant, and the effective potential $V_{\text{eff}}(a)$ is given by

$$V_{\text{eff}}(A) = -\mu \left(\frac{1}{4}A^2 - \frac{1}{32}A^4 + \frac{\alpha}{96}A^6 - \frac{5\beta}{1024}A^8 + \frac{E_0}{2\omega}A \right) - \frac{\tilde{D}}{2}\ln(A). \quad (35)$$

To analyze the effect of the deterministic excitation on the escape rates ($T_{1,3}$) of right limit-cycle A_3 and the left stable limit-cycle A_1, we consider again the mean exit time

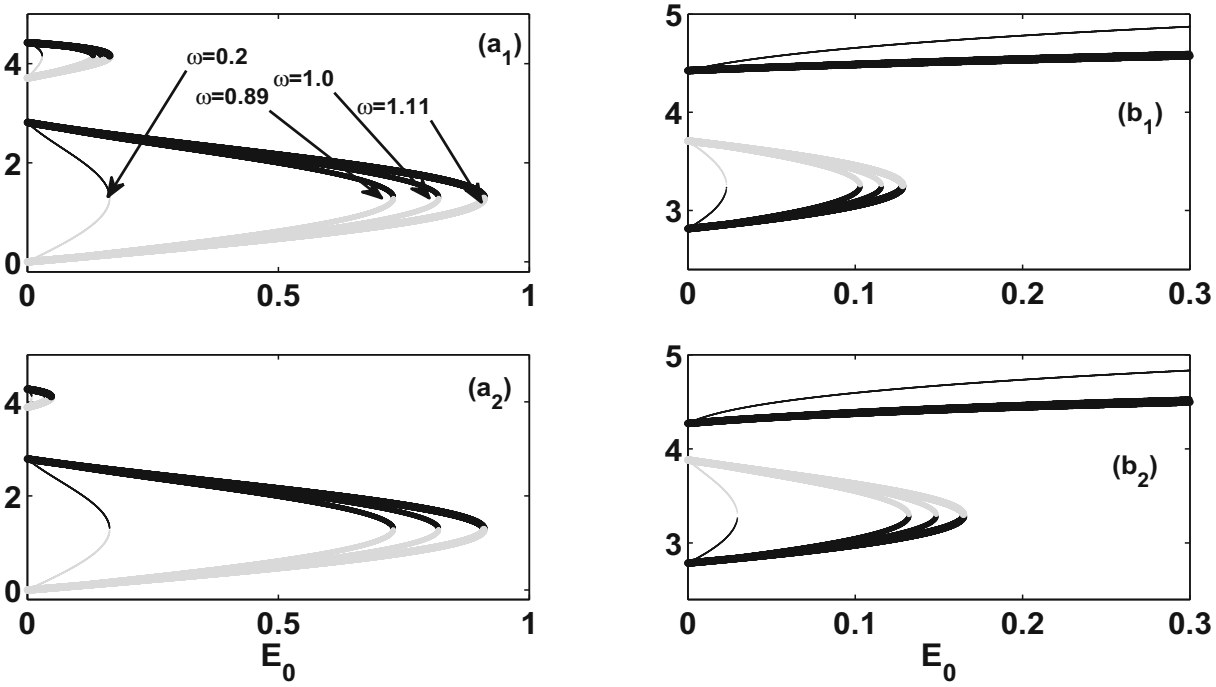

Fig. 6. Behavior of amplitude versus strength E_0 of the driving force in the stochastic average approximation, for: ($a_{1,2}$): $\phi = \frac{\pi}{2}$, ($b_{1,2}$): $\phi = -\frac{\pi}{2}$, and for different frequencies of external excitation. The parameters top $\alpha = 0.1547$, $\beta = 0.006$, bottom $\alpha = 0.154$, $\beta = 0.006$. The nonlinear parameter reads $\mu = 0.001$.

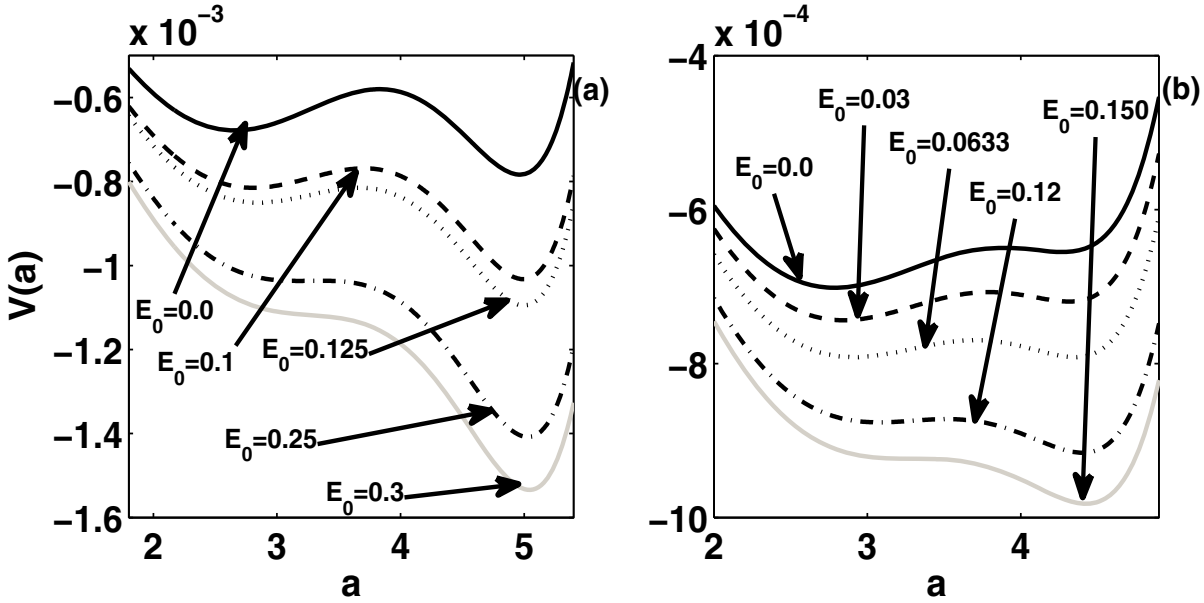

Fig. 7. Behavior of the quasi-potential $V(a)$ as function of amplitude a with different strengths E_0 of the driving force in the stochastic average approximation. The parameters left (a) $\alpha = 0.145$, $\beta = 0.005$, right (b) $\alpha = 0.154$, $\beta = 0.006$. The nonlinear parameter reads $\mu = 0.001$.

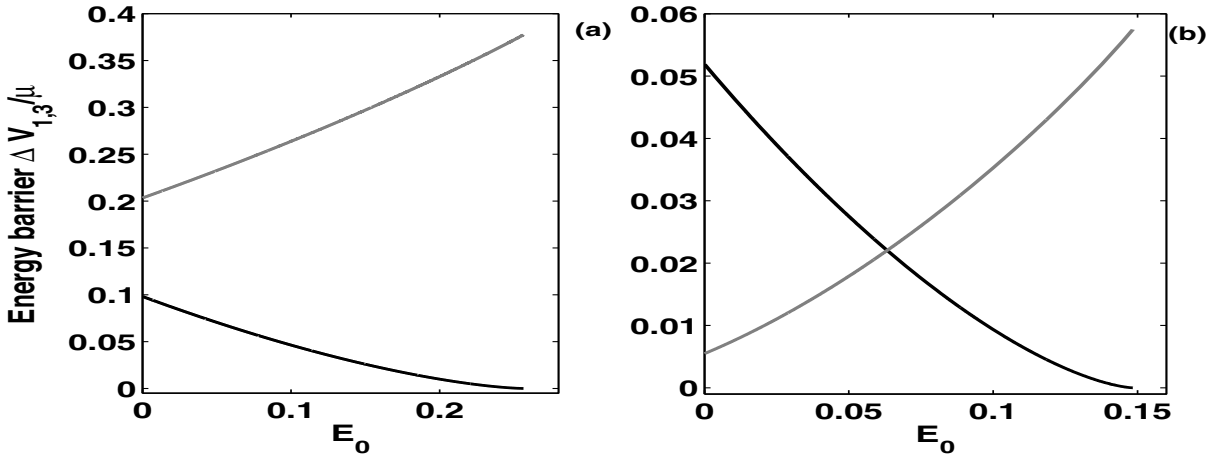

Fig. 8. Behavior of the quasipotential energy barriers versus driving force intensity E_0 in the stochastic average approximation. Black lines denote the ΔV_1 and grey light lines denote the ΔV_3. The parameters of the system are: (a) $\alpha = 0.145$, $\beta = 0.005$, (b) $\alpha = 0.154$, $\beta = 0.006$. The nonlinear parameter reads $\mu = 0.001$.

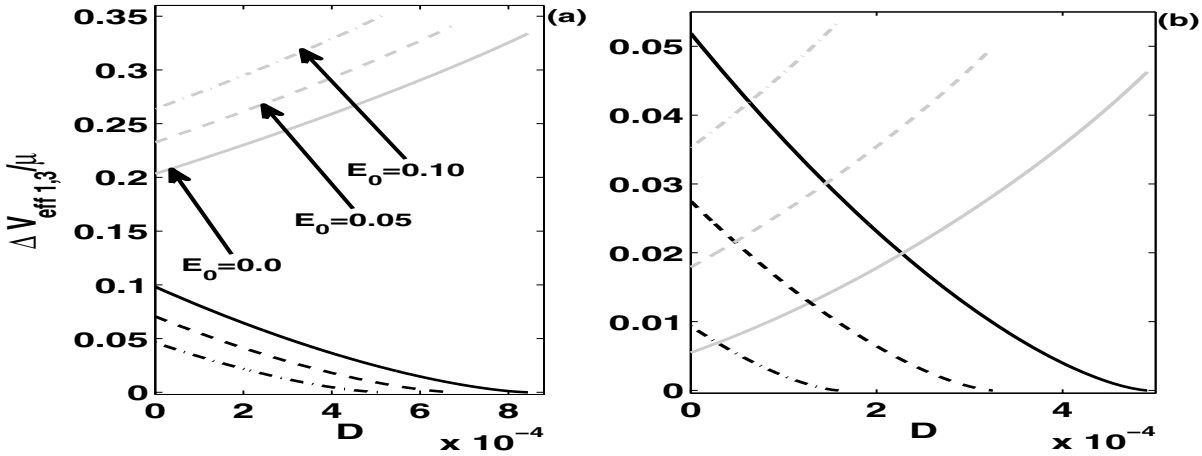

Fig. 9. Behavior of the quasipotential energy barrier versus noise intensity D for different values of driving force intensity E_0 in the stochastic average approximation. The black lines denote the $\Delta V_{\text{eff}1}$ and grey light lines denote the $\Delta V_{\text{eff}3}$. The parameters of the system are: (a) $\alpha = 0.145$, $\beta = 0.005$, (b) $\alpha = 0.154$, $\beta = 0.006$.

of the system from different well of the effective potential $V_{\text{eff}}(A)$. When $\tilde{D}$ is small in comparison with the height of the energy barrier [12,18], i.e., $\tilde{D} < \mid V_{\text{eff}}(A_2) - V_{\text{eff}}(A_{1,3}) \mid$. Through equation (35) one can derive the behavior of the effective potential barriers $\Delta V_{\text{effi}}(a)$ [12,18]. In fact, if one approximates the full birhythmic behavior with an effective Brownian motion of the particle in a double well potential, the effective potential barriers can be considered as an energy needed to escape from an orbit to the other. The analytic predictions of the energies $\Delta V_{\text{eff}1}$ and $\Delta V_{\text{eff}3}$ as a function of noise intensity D for different deterministic intensities E_0 are shown in Figure 9.

As in reference [43], due to the shape of Figure 7, the probability distribution is in general very asymmetric; for fixed parameters α, β the probability distribution function $p(A)$ can be localized around a single orbit. For the set of parameters (α, β) in the gray area (the case of an asymmetrical potential) in Figure 1, one notes that a sudden qualitative change of $p(a)$ in the presence of noise, is denoted as P-bifurcations [43]. This can be seen in Figure 10 that the distribution with two peaks evolves into one peaks as the noise intensity D changes gradually.

5.2 Numerical investigation of the response to a sinusoidal drive

In stochastic resonance, besides the analysis of escape times as indicators of coherence, it is important to reconstruct at least the qualitative properties of the system as a detector. In this framework, one interprets the deterministic term in equation (18) as a signal to be revealed analysing the response of the van der Pol oscillating system, and noise is the disturbing term that hinders the detection. A standard tool to characterize the signal enhancement due to noise is the SNR, as per equation (18).

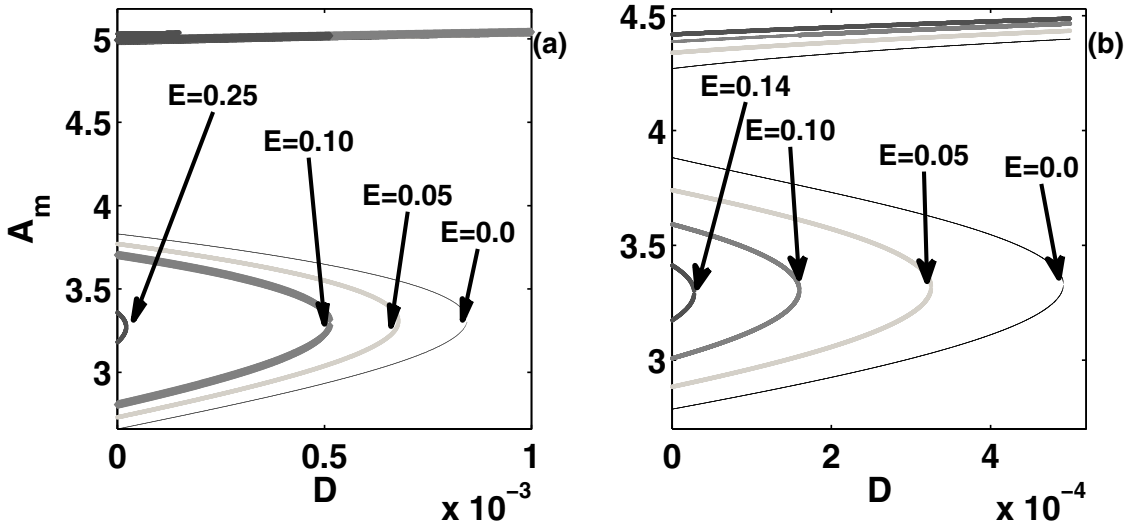

Fig. 10. Evolution of most probable amplitude of limit cycle versus the noise intensity D, with different strengths E_0 of the driving force in the stochastic average approximation. The parameters are: (a) $\alpha = 0.145$, $\beta = 0.005$, (b) $\alpha = 0.154$, $\beta = 0.006$. The nonlinear parameter reads $\mu = 0.001$.

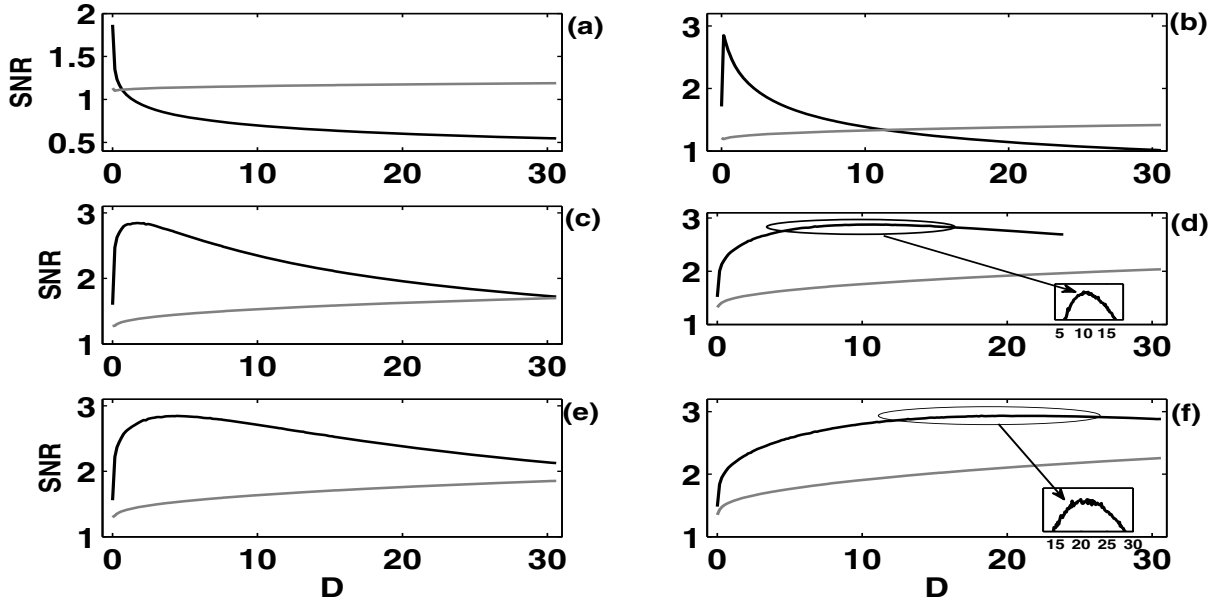

Fig. 11. The signals-to-noise ratio versus noise intensity D for different values of (α, β) chosen in the symmetric area of Figure 1: (a): $\alpha = 0.0675$; $\beta = 0.0009$; (b): $\alpha = 0.12$; $\beta = 0.0032$; (c): $\alpha = 0.1476$; $\beta = 0.0053$; (d): $\alpha = 0.16$; $\beta = 0.00658$; (e): $\alpha = 0.1547$; $\beta = 0.006$; (f): $\alpha = 0.1635$; $\beta = 0.007$. The other parameters read $E_0 = 0.1$, $\omega = 0.2$, $\mu = 0.001$.

To obtain an estimate of such enhancement, we have simulated the van der Pol system at a fixed the value of external drive frequency, $\omega = 0.2$ – a value where the analytic approximation of Section 5.1 is not valid, for it assumes $\omega \simeq \Omega$. Averaging over 200 realizations for as long as 10^6 normalized time units and in the so-called coherent detection [41,42], i.e. the case where the initial state of the detector (in our case, the vdP oscillator) is fixed and influences the signal detection. The investigation of the interplay between noise and the coherent driving input gives rise to the phenomenon of stochastic resonance.

Figure 11 shows the SNR as a function of D in an area of approximately symmetric potential for $E_0 = 0.1$, $\omega = 0.2$, and $\mu = 0.001$ with different initial condition (black: IC is around the inner orbit A_1; gray curve: IC is around the outer orbit A_3). In Figure 11a, the SNR shows no peak for both ICs. It is evident that SR does not occur with the corresponding set of parameters $\alpha = 0.0675$, $\beta = 0.0009$. Figures 11b–11f display the response of the system when it appears a resonant-like behavior as a function of the noise level, that is a signature of SR. A stochastic resonance-like phenomenon is only observed when the system starts

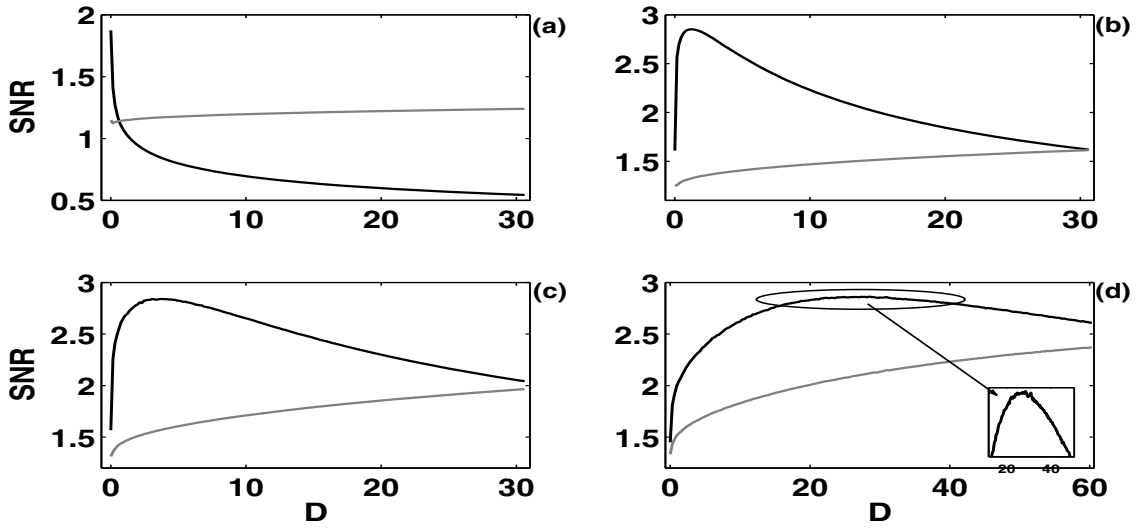

Fig. 12. The signals-to-noise ratio versus noise intensity D for different values of (α, β) chosen in the Asymmetric area in Figure 1: (a): $\alpha = 0.0675$; $\beta = 0.0009$; (b): $\alpha = 0.12$; $\beta = 0.0032$; (c): $\alpha = 0.1476$; $\beta = 0.0053$; (d): $\alpha = 0.16$; $\beta = 0.00658$. The other parameters read $E_0 = 0.1$, $\omega = 0.2$, $\mu = 0.001$.

on the inner orbit with a low value of the parameter of nonlinearity, μ.

In the area where an asymmetric potential is expected (see Fig. 1), the analysis shows some analogous features, as displayed in Figure 12 at $E_0 = 0.1$, $\omega = 0.2$ and $\mu = 0.001$. In Figure 12a there is no SR-like phenomenon, while in Figures 12b–12d the SNR as a function of D exhibits a maximum for an optimal noise intensity, a characteristic feature of SR phenomena. It is clear that no SR occurs when the system starts around the outer orbit A_3.

6 Conclusion

We have investigated the effect of noise added to a forced birhythmic van der Pol-like system that describes some applications as, e.g., enzymatic reactions, sleep-awake cycles, and energy harvesting. The interest also arises from the interplay between the time scales: the two oscillations periods (that are the essence of birhythmicity), the drive frequency (that is externally controlled), and the noise induced average escape time (that is determined by the quasi-potential). Moreover, the system is also analytically convenient. In fact, using the method of stochastic averaging, one can reduce the modified van der Pol equation (3) to an asymmetric bistable system driven by Gaussian white noise.

In the stochastic averaging approximation the two orbits correspond to two fix points, and the stability (in the low noise limit) can be estimated through the quasi-potential, also in the presence of a forcing term at a frequency close to the frequency of self-oscillations. The numerical analysis reveals several features of the driven birhythmic system:

(a) The ACF shows that the dominating time scale is dictated by the activation energy (as derived by the quasi-potential) and not by the spontaneous oscillations periods, Figure 3.
(b) There is a special value for the noise D_c at which the ACF reaches a minimum, a signature of anti-correlation. The D_c values are slightly different for the inner and outer orbit, Figure 4.
(c) The escape times distribution (as measured by the coefficient of variation CV or equivalently by the effective diffusion constant D_{eff}) depends upon the self generated oscillations of the birhythmic van der Pol, Figure 5.

One concludes that the different tools to characterize the system are sensitive to different phenomena, ACF to (rare) escapes from the stable orbits, the escape times to the oscillations of the attractors. Thus, the escapes from the quasi-potential behave as expected for an ordinary potential, but they also keep memory of the fact that the system is in fact oscillating (the stable point in the averaged system represents an orbit) and can (stochastically) resonate also at the orbit frequency.

The analytical treatment (by means of stochastic averaging) allows to estimate the behavior of the quasi-potential (or the effective activation energies, V in Fig. 7) as a function of the drive amplitude (Fig. 8) and of the white noise intensity (Fig. 9). The analysis reveals that the drive amplitude can either increase or decrease the stability of the orbits. Instead, the noise amplitude always tends to stabilize the outer orbit (i.e., to increase the effective activation energy) and to weaken the stability of the inner orbit (i.e., to decrease the effective activation energy). This type of analysis can only be performed for a drive frequency that is close to the oscillation frequency. As the stochastic averaging is only applicable when the drive frequency is equal to the oscillator frequency, we have employed numerical simulations to evaluate the SNR for slow frequency (respect to the natural frequency of the van der Pol oscillator), in the so called coherent detection

approach, that keeps memory of the initial conditions. The SNR associated to a small periodic drive shows markedly different properties if the initial conditions are selected on the inner or outer orbit: depending on the parameter set, stochastic resonance is observed either for the inner or for the outer orbits. This is compatible with a picture of bistable oscillations between the two stable orbits. However, it remains to be established if the incoherent detection case, where the average washes out the influence of the initial conditions, also exhibits stochastic resonance.

R.Y. undertook this work with the support of the Max Planck Society, Germany. He acknowledges the support of the Max Planck-Institut of Mathematical Sciences, Leipzig, Germany.

G.F. acknowledges financial support from "Programma regionale per lo sviluppo innovativo delle filiere Manifatturiere strategiche della Campania Filiera WISCH: Progetto2: Ricerca di tecnologie innovative digitali per lo sviluppo sistemistico di computer, circuiti elettronici e piattaforme inerziali ad elevate prestazioni ad uso avionico". Open access funding provided by Max Planck Society.

Author contribution statement

This paper was proposed by Prof R. Yamapi and Prof. G. Filatralla. C. Chéagé Chamgoué is the main author of the paper, while Prof. P. Woafo was the supervisor of this works.

References

1. Y.-X. Li, A. Goldbeter, J. Theor. Biol. **138**, 149 (1989)
2. M.E. Jewett, D.B. Forger, R.E. Kronauer, J. Biol. Rhythms **14**, 493 (1999)
3. C. Suguna, S. Sinha, Fluct. Noise Lett. **2**, L313 (2002)
4. I. Potapov, E. Volkov, A. Kuznetsov, Phys. Rev. E **83**, 031901 (2011)
5. J. Hounsgaard, H. Hultborn, B. Jespersen, O. Kiehn, J. Physiol. **405**, 345 (1988)
6. N. Geva-Zatorsky, N. Rosenfeld, S. Itzkovitz, R. Milo, A. Sigal, E. Dekel, T. Yarnitzky, Y. Liron, P. Polak, G. Lahav, U. Alon, Mol. Syst. Biol. **2**, 2006.0033 (2006)
7. B. Van der Pol, J. Van der Mark, Nature **120**, 363 (1927)
8. B. van der Pol, J. van der Mark, Philos. Mag. Ser. **7**, 6 (1928)
9. R. Yamapi, Physica A **366**, 187 (2006)
10. A. Zakharova, T. Vadivasova, V. Anishchenko, A. Koseska, J. Kurths, Phys. Rev. E **81**, 011106 (2010)
11. P. Ghosh, S. Sen, S.S. Riaz, D.S. Ray, Phys. Rev. E **83**, 036205 (2011)
12. R. Yamapi, G. Filatrella, M.A. Aziz-Aloui, Chaos **20**, 013114 (2010)
13. F. Kaiser, Biol. Cybernet. **27**, 155 (1977)
14. F. Kaiser, in *Coherent Excitations in Biological Systems*, edited by H. Frhlich, F. Kremer (Springer-Verlag, Berlin, 1983), pp. 128–133
15. H. Fröhlich, in *The Fluctuating Enzyme*, edited by G.R. Welch (Wiley, New York, 1986), p. 421
16. V.-X. Li, A. Goldbeter, J. Theor. Biol. **138**, 149 (1989)
17. F. Kaiser, C. Eichwald, Int. J. Bifurc. Chaos Appl. Sci. Eng. **1**, 485 (1991)
18. A. Chéagé Chamgoué, R. Yamapi, P. Woafo, Eur. Phys. J. Plus **127**, 59 (2012)
19. D. Biswas, T. Banerjee, J. Kurths, Phys. Rev. E **94**, 042226 (2016)
20. H.A. Kramers, Physica **7**, 284 (1940)
21. P. Hänggi, P. Talkner, M. Borkovec, Rev. Mod. Phys. **62**, 251 (1990)
22. R.L. Stratonovich, *Selected Problems of Fluctuation Theory in Radiotechnics* (Sov. Radio, Moscow 1961) (in Russian), Selected Topics in the Theory of Random Noise (Gordon and Breach, New York, 1963, 1967), Vols. 1, 2
23. R.F. Grote, J.T. Hynes, J. Chem. Phys. **73**, 2715 (1980)
24. A. Longtin, A. Bulsara, D. Pierson, F. Moss, Biol. Cybern. **70**, 569 (1994)
25. M.I. Dykman, M.A. Krigovlaz, Sov. Phys. JETP **50**, 30 (1979)
26. R. Graham, T. Tél, Phys. Rev. A **31**, 1109 (1985)
27. R. Graham, in *Instabilities and Nonequilibrium Structures*, edited by E. Tirapegui, D. Villarroel (Reidel, Dordrecht, 1987), pp. 271–290, 435
28. H.S. Wio, R.R. Deza, J.M. Lopez, *An Introduction to Stochastic Processes and Nonequilibrium Statistical Physics*, revised edn. (World Scientific, Singapore, 2012)
29. R.L. Kautz, J. Appl. Phys. **76**, 5538 (1994)
30. R. Yamapi, G. Filatrella, M.A. Aziz-Alaoui, H.A. Cerdeira, Chaos **22**, 043114 (2012)
31. R. Mbakob Yonkeu, R. Yamapi, G. Filatrella, C. Tchawoua, Physica A **466**, 552 (2017)
32. R. Mbakob Yonkeu, R. Yamapi, G. Filatrella, C. Tchawoua, Nonlinear Dyn. **84**, 627 (2016)
33. R. Mbakob Yonkeu, R. Yamapi, G. Filatrella, C. Tchawoua, Commun. Nonlinear Sci. Numer. Simul. **33**, 70 (2016)
34. S. Hartzell, M.S. Bartlett, L. Virgin, A. Porporato, J. Theor. Biol. **368**, 83 (2015)
35. A. Fiasconaro, A. Ochab-Marcinek, B. Spagnolo, E. Gudowska-Nowak, Eur. Phys. J. B **65**, 435 (2008)
36. R. Yang, A. Song, Int. J. Mod. Phys. B **22**, 5365 (2008)
37. L. Gammaitoni, P. Hänggi, P. Jung, F. Marchesoni, Rev. Mod. Phys. **70**, 223, (1998)
38. Th. Wellens, V. Shatokhin, A. Buchleitner, Rep. Prog. Phys. **67**, 45 (2004)
39. C. Stambaugh, H.B. Chan, Phys. Rev. B **73**, 172 (2006)
40. M. Gitterman, *The Noisy Oscillator: The First Hundred Years, From Einstein Until Now* (World Scientific, Singapore, 2005)
41. P. Addesso, G. Filatrella, V. Pierro, Phys. Rev. E **85**, 016708 (2012)
42. P. Addesso, V. Pierro, G. Filatrella, Commun. Nonlinear Sci. Numer. Simulat. **30**, 15 (2016)

43. A. Chéagé Chamgoué, R. Yamapi, P. Woafo, Nonlinear Dyn. **73**, 2157 (2013)
44. V.S. Anishchenko, V. Astakhov, A. Neiman, T. Vadivasova, L. Schimansky-Geier, *Nonlinear Dynamics of Chaotic and Stochastic Systems: Tutorial and Modern Developments* (Springer, Berlin, 2007)
45. H.G. Enjieu Kadji, J.B. Chabi Orou, R. Yamapi, P. Woafo, Chaos Solitons Fract. **32**, 862 (2007)
46. H.G. Enjieu Kadji, R. Yamapi, J.B. Chabi Orou, Chaos **17**, 033113 (2007)
47. H. Risken, *The Fokker-Planck Equation: Methods of Solution and Applications* (Springer, Berlin, 1989)
48. C. Gardiner, *Handbook of Stochastic Methods for Physics, Chemistry and the Natural Sciences* (Springer, Berlin, 2004)
49. A.S. Pikovsky, J. Kurths, Phys. Rev. Lett. **78**, 775 (1997)
50. B. Lindner, L. Schimansky, Phys. Rev. E **61**, 6103 (2000)
51. M.C. Mahato, S.R. Shenoy, Phys. Rev. E **50**, 2503 (1994)
52. B. Lindner, L. Schimansky-Geier, Phys. Rev. E **60**, 7270 (1999)
53. B. Lindner, J. Garcia-Ojalvo, A. Neiman, L. Schimansky-Geier, Phys. Rep. **392**, 321 (2004)
54. A. Papoulis, S.U. Pillai, *Probability, Random Variables, and Stochastic Processes*, 4th edn. (McGraw-Hill, Boston, 2002)
55. G. Litak, M.I. Friswell, S. Adhikari, Appl. Phys. Lett. **96**, 214103 (2010)
56. G. Litak, M. Borowiec, Nonlinear Dyn. **77**, 681 (2014)
57. R. Guantes, G.G. de Polavieja, Phys. Rev. E **71**, 011911 (2005)
58. N. Krylov, N. Bogoliubov, *Introduction to nonlinear mechanics* (Kiev, 1931), transl. by S. Lefschetz, Annals Math. Studies No. 11 (Princeton Univ. Press, Princeton, 1943)
59. P. Hanggi, P. Riseborough, J. Am. Phys, **51**, 347 (1983)
60. C.S. Manohar, R.N. Iyengar, Int. J. Non-Linear Mech. **26**, 679 (1991)
61. V.M. Gandhimathi, K. Murali, S. Rajasekar, Physica A **347**, 99 (2005)
62. V.M. Gandhimathi, K. Murali, S. Rajasekar, Chaos Solitons Fract. **30**, 1034 (2006)